

# Case Study of Vertical Slope Excavation Near Existing Buildings based on Visual Monitoring of Intelligent Robots

Kun Yuan<sup>1</sup>, Yufang Zhang<sup>1</sup>, Shangyi Zhao<sup>1\*</sup>, Gaoxiang Zheng<sup>2</sup>, Yaqiong Xie<sup>2</sup>

<sup>1</sup>China Railway Science Research Institute, Beijing, China

<sup>2</sup>Chongqing Jiaotong University, Chongqing, China  
zhaoshangyi2021@126.com

**Abstract**— Case study of the vertical slope excavation near existing buildings based on visual monitoring of intelligent robots is conducted in the paper. A recent development in Western China required the excavation and vertical cut of a rock slope, which might cause large deformation or failure of existing buildings above the slope. The minimum horizontal distance between the buildings and the cut edge of the slope was 3 meters and the maximum excavation depth was 20 meters. The rock slope was composed of soil, weathered mudstone, sandstone and a set of bedding planes indining outward was observed. Stabilizing piles strengthened by a series of tie-back anchors were designed to protect the cut slope. The lateral loads acting on the anchor cable and piles was determined by maximal value of the at-rest pressure and modified active pressure. It was observed that the construction sequence had a significant impact on the stability of the slopes. To achieve the efficient computer based analysis, the novel visual monitoring system and intelligent robot is combined. The motion control system of the intelligent robot controls the machine equipment and performs industrial operations and the core of the intelligent robot is the motion control system. A novel motion control algorithm is designed to deal with the challenges in complex scenarios. Through the testing on various applications, the robustness is validated.

**Keywords**— Intelligent robots; visual monitoring; data mining; vertical slope excavation; smart buildings

## I. INTRODUCTION

Deep vertical cut of slopes are often conducted for projects located in densely populated urban areas. The cut may cause the lateral displacement or failure to the foundations of existing buildings and therefore the safety of the buildings is a major concern in vertical cut projects [1, 2, 3]. A number of well-documented case histories have been reported

The performance of a high cut slope and adjacent structures is related to both the stability and deformation. Predicting building damage due to ground deformations caused by deep excavations is an important design consideration in a congested urban environment. The bracing system and adjacent building must meet both ultimate and serviceability limit state requirements. The key issue is how to estimate the deformations and the corresponding lateral loads acting on the retaining structure. Stability safety factor can be calculated with traditional limit equivalent method whereas deformations are more difficult to predict accurately due to the limitation of the constitutive models of rocks and soils. The

excavation-induced deformations involves a combination of geotechnical and structural aspects, such as green field displacements, building behaviour, soil – foundation - building interaction [4, 5, 6, 7].

The deformation depend on the geology conditions, relative stiffness of the building and the interface between soil and building, retaining schemes and the methods of construction (e.g. top-down, bottom-up excavation sequences) [8, 9, 10]. Modelling this effect with both soil and building in a combined calculation is still not well developed.

Many theoretical and empirical methods have been established for solving certain types of excavation problems. Current predictive approaches consist of empirical methods, advanced numerical analysis, and field monitoring. In most of the cases, the geotechnical material mainly consists of soil. For the rock cut slope, the effect of deep excavation on adjacent buildings have not been studied enough [11, 12, 13]. The present paper introduces a case study of a high rock cut slope in Western China. The empirical methods, the induced failure of retaining schemes and construction sequences are discussed. It shows that the top down construction sequences have significant impact to the deformation of the cut wall. Using the stabilizing piles with cable anchors is one of the reliable retaining schemes for the high cut rock slope which is close to the existing building. The lateral loads acting on the retaining structure can be determined by the maximal value of the at-rest pressure and modified active pressure [14, 15].

Hence, for the comprehensive analysis, we will integrate the visual monitoring of intelligent robots. From a theoretical point of view, intelligent manufacturing is different from artificial intelligence in the general traditional sense. The characteristics of intelligent manufacturing technology are that it assists mechanical production, management call-out and production control. In terms of the basic autonomous technical processing capabilities, intelligent manufacturing can be based on manual intervention to realize the monitoring of the whole production process and minimize the general cost of labor management and production monitoring [16, 17, 18]. The pressure sensor has the functions of detection and information processing. It will feel the pressure signal, and according to certain rules, the analog quantity of the pressure signal will be converted into a digital quantity and finally used by the controller.

Of course, when the design of a smart device is not only about the intelligence of the processor, but also needs to be intelligentized in all parts, and finally all parts are integrated to obtain a smart device. Hence the need for an intelligent pressure sensor is essential, and also the integration of the visual information system is also important. The integrated monitoring system of building equipment consists of three layers of equipment and two layers of network structure, which are divided into station control layer, communication management layer and field control layer [19, 20, 21].

The station control layer and the basic communication management layer are connected through TCP/IP Ethernet, and the communication management layer and the field control layer are connected through a fieldbus network to realize remote monitoring and management of decentralized building equipment, the figure 1 shows the details [22, 23].

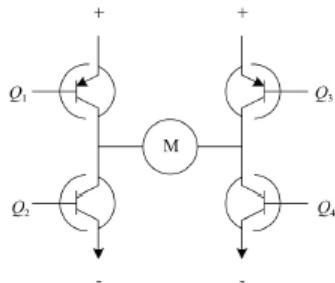


Fig. 1. The Basic Structure of the Intelligent Robots

## II. THE RELATED WORK AND BACKGROUND

In this section, we focus on the monitoring system and the vertical slope excavation near existing buildings modelling [24, 25, 26].

Cameras are installed on construction sites as the main monitoring method. At the same time, as an auxiliary method, mobile phones can also be used to take pictures for visual monitoring management combined with traditional manual supervision. Construction site safety technicians conduct the safety supervision through some safety monitoring data [27, 28, 29]. For the construction of each sub-project, they will take pictures and upload them to the visual safety monitoring system from time to time to check for potential safety hazards. Security incidents provide the basis for incident analysis.

The field control layer is composed of the decentralized integrated monitoring devices for construction equipment to realize the local automatic control of construction equipment. At the same time, all the information of the integrated control device is sent to the core communication management layer through the fieldbus and receives various control instructions from the communication management layer. The Web server side and the database form a three-tier structure. When using the B/S architecture for software system development, only a specific browser is required, and the requirements for users are not high, and the Web browser only handles the corresponding work of the display logic.

Processing the main logical transactions, based on this, the cost of the client can be reduced. Since the client has little logical content, it becomes a thin client. Since the client uses a

browser, the interface is still simple and the operation is convenient, and no other software needs to be installed takes up less memory. The wireless communication module is connected with the controller in the form of serial port, which transmits the packaged data to the user server through the network operator, and the server software writes the data into the data table corresponding to the database according to the format after data processing. Users can view environmental parameters and device status through the website integrated monitoring platform and Android mobile phone monitoring software. A new real estate projects were developed in Chongqing, China, which caused a large and deep excavation near the existing buildings. The minimum horizontal distance between the buildings and the cut edge of the slope was 3 meters and the maximum excavation depth was 20 meters. It might cause the deformation or failure of existing buildings above the slope. The new construction project consists of two 30 storey building.

As shown in Figure 2, on top of the slope there were many existing buildings that were supported on strip foundations placed on the highly weathered bedrock layer. Figures 3 and 4 show the plan view of the cut slope and the cross section of 1-1 respectively [30].



Fig. 2. The Old Buildings on Top of Slope

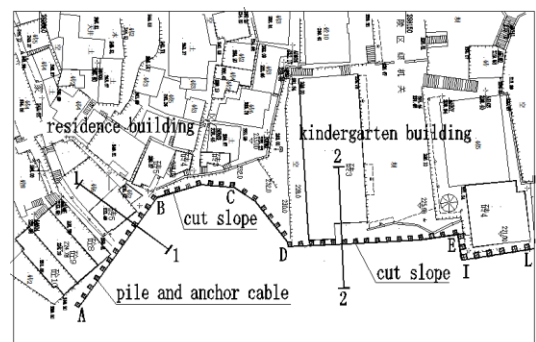


Fig. 3. The Plan view of cut slope

The material at this site mainly consists of artificial soil layer, mudstone and sandstone.

Mudstone: thick layered structure, occasionally holding a layer of thin sandstone and grey green rock.

Sandstone: thick layered structure, locally containing mudstone.

The upper highly weathered layer: broken rock, crack development.

The lower part of medium weathered layer: stratified rock, drill core sample remain relatively intact, locally crushed, fissured.

There are two sets of joints in the bedrock:

①orientation  $195^{\circ} \angle 63^{\circ}$ , length 0.5m~1.5m, relatively straight and a closed form, spacing 1m~2m, rigid rough surfaces, combined poorly.

②orientation  $105^{\circ} \angle 79^{\circ}$ , length 0.5m~1m, in a closed state, spacing 6m~1.2m, rigid rough surface, combined poorly.

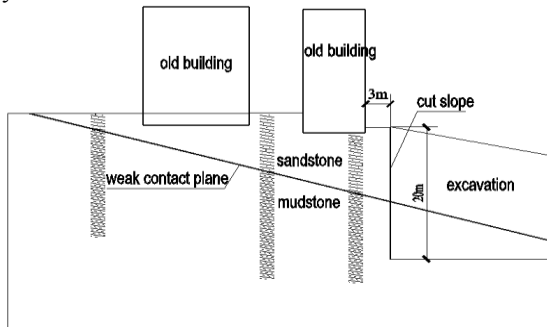


Fig. 4. The Cross-sectional view of the Section 1-1

The field investigation revealed that there was a weak bedding plane between the sandstone and mudstone. The weak interlayer was filled with clay. Because of low permeability of mudstone, groundwater accumulated in the bedding plane and therefore reduced the shear strength of the bedding plane significantly. According to the test result, the cohesion of the bedding plane is 20kPa and internal friction angle is  $12^{\circ}$ . The dip angle of the bedding plane is  $15^{\circ}$  as shown in Figure 4.

The dip direction of bedding plane is  $35^{\circ}$ , inclination of  $15^{\circ}$ . The cohesion of bedding plane and joints surface is 50kPa, internal friction angle is  $18^{\circ}$ .

By the analysis of stereographic projection as shown in Figure 5, the rock mass was likely to slide along the outward-dipping plane of the bedding plane and the weak contact plane.

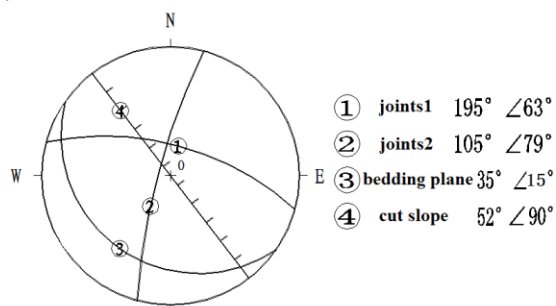


Fig. 5. The Stereographic projection of structure plane

The Chinese technical code (references GB 50330 -2013) for building slope engineering classifies the rock mass into four categories according to rock mass structure characterization such as the integrity coefficient, combination condition, orientation and stability of vertical slope. The equivalent internal friction angle are suggested in the Chinese technical code for building slope engineering as shown in table 1.

Table 1. Equivalent internal friction angle of different class of rock mass

class of rock mass	I	II	III	IV
equivalent internal friction angle ( $^{\circ}$ )	$\varphi_e \geq 72$	$72 \geq \varphi_e > 62$	$62 \geq \varphi_e > 52$	$52 \geq \varphi_e > 42$

The equivalent internal friction angle is an imaginary internal friction angle without consideration of the cohesion. According to rock mass structure and characterization of the field, the class of rock mass is III. The suggested equivalent internal friction angle is  $55^{\circ}$ . According to the survey report, The design parameters from the survey report are shown in table 2.

Table 2. Parameters selected for numerical simulations

Materials	soil	sandstone		mudstone	
		highly-weathered	medium-weathered	highly-weathered	medium-weathered
Unit weight (kN/m <sup>3</sup> )	20.5	23	26.0	23	25.2
Internal friction angle( $^{\circ}$ )	30	28	34	26	29
Cohesion (kPa)	5	60	1650	50	280
Elastic modulus (MPa)			1960		1160
Poisson's ratio	0.45		0.29		0.34
Integrity coefficient of rock mass			0.63~0.71		0.63~0.71
Characteristic value of bond strength between grout and rock (kPa)		100	550	80	150

### III. THE PROPOSED METHODOLOGY AND VERIFICATION

#### A. The Smart Robot Model

An intelligent robot is a device that realizes intelligent industrial production based on the imitation of human motion control principles. The motion control system of the intelligent robot controls the machine equipment and performs industrial operations and the core of the intelligent robot is the motion control system.

The motion control of intelligent robots consists of two parts: hardware and software. The Arduino IDE is a key platform for software development of intelligent robotic toys. First, you should configure the corresponding driver according to the serial port type. After the driver is installed, you can see the installed port number in the control panel. In addition, enter the Arduino platform, select the corresponding board and port number in the toolbar, and write, debug and download the software code after the board and port number are configured. The robot system design scheme based on EMC intelligent auxiliary measurement mainly includes two parts: the design of the robot's workflow and the division of the robot's functional modules.

Among them, for the design of the robot workflow, taking the test of the intelligent auxiliary ranging robot as an example, first, after starting the intelligent auxiliary test robot, the robot should be tested in-situ, and the in-situ position coordinates of the robot should be calibrated; Through intelligent auxiliary ranging robot program debugging, the robot can move the corresponding distance (set distance) according to the core direction and speed set by the original program, and at the same time, the distance detection is carried out through the ranging sensor to ensure that the robot can finally reach the most effective detection point and again, after determining that the robot reaches the effective detection point, detect the specific distance between the rangefinder sensor on the robot and the front end of the rangefinder.

When the distance between the rangefinder and the rangefinder sensor is within 2 mm Within, the entire robot system defaults to this distance as the safety test distance. For the system, we should consider the 2 core aspects as follows.

(1) Intelligent manufacturing technology has some certain performance requirements for application sensor technology. The three most important indicators are refresh rate, dynamic capture accuracy and information feedback delay. The refresh rate refers to the frequency that the sensor can process the image information of the monitoring range within a fixed period of time, to ensure that the sensor can use the shortest time to feedback the information content within a limited period of time to control the time cost of the technology application.

(2) The signal transmission and general processing of mechatronics technology is based on electrical signals. From technical content, mechatronics and intelligent manufacturing technology are not interconnected. However, from the basic perspective of technical principle, the application of modern mechatronics technology can also realize the application of network transmission information based on external server and terminal system. Therefore, in some terms of the intelligent manufacturing technology, we can then use the mechatronics electrical signal transmission platform to realize the simulation of network transmission information, and realize the effective application of intelligent manufacturing technology to signal processing technology based on digital signal.

### B. The Theoretical Analysis

According to geological conditions, there are several potential failure mode after excavation as follow.

1) Sliding along the outward-dipping structural plane. The possible sliding plane include bedding plane and sandstone and mudstone contact surface as shown in Figure 6.

2) Sliding along the Coulomb failure surface that the sliding plane will pass through the toe (see Figure. 6) and inclines at an angle of  $45^\circ + \varphi/2 = 63^\circ$ .

3) Deformation and crack in existing old building structure.

The slope stability analysis was carried out using Spencer's method of slices and shear strength reduction method.

Strength reduction means reducing the parameters of shear strength (cohesion and internal friction angle) of soil (or rock) slopes in the numerical calculation, within an elastic-perfectly plastic constitutive models, until the limit failure state is reached. The shear strength is reduced according the Mohr Coulomb yield criteria as follows:

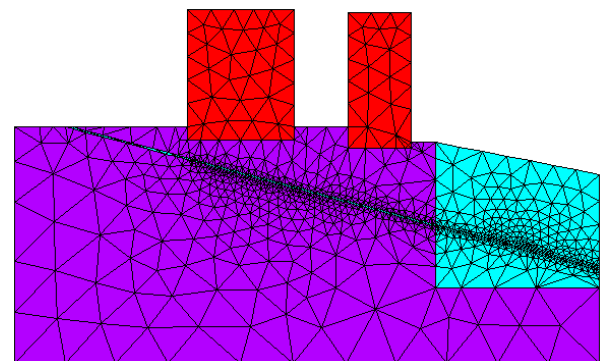
$$c' = \frac{c}{F_s}, \tan \varphi' = \frac{\tan \varphi}{F_s} \quad (1)$$

Then, the sliding surface of the slope can be automatically obtained from the results of numerical calculation and the stability safety factor can be calculated. The ratio between the actual strength and the model strength at the stability limit is the stability safety factor. For Mohr Coulomb yield criteria, the  $F_s$  of the strength reduction method can be expressed as follows:

$$F_s = \frac{c}{c'} = \frac{\tan \varphi}{\tan \varphi'} \quad (2)$$

According to calculation result, the stability safety factor is 1.69 when the rock mass sliding along the bedding plane. It is greater than the desired value 1.4. It shown that rock mass can't slide along the bedding plane.

The stability safety factor is 1.06 when the rock mass slides along the weak contact surface of sandstone and mudstone. Although the safety factor is greater than 1.0, it is less than the design safety factor 1.4. So, it needs to be reinforced. Figure 6 shows the failure model of rock mass slide along the weak contact surface using the strength reduction finite element method. It shows that rock mass slide along the sandstone and mudstone contact surface when the reduction coefficient is up to 1.06.





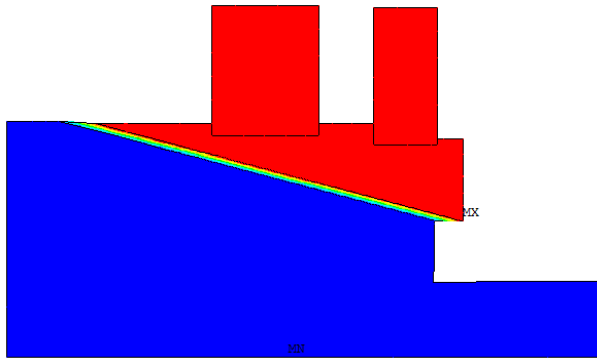


Fig. 6. The Rock mass slide along the weak contact surface

The factor of safety is 1.87 using the medium weathered rock mass shear strength without considering outward-dipping structural plane. Figure 7 shows the failure model when the reduction coefficient is up to 1.87. It showed that the rock mass can't slide along the Coulomb failure surface. But if we use highly-weathered rock mass shear strength, factor of safety reduced to 0.87. It showed that the highly-weathered rock slope can't keep stable without support in time.

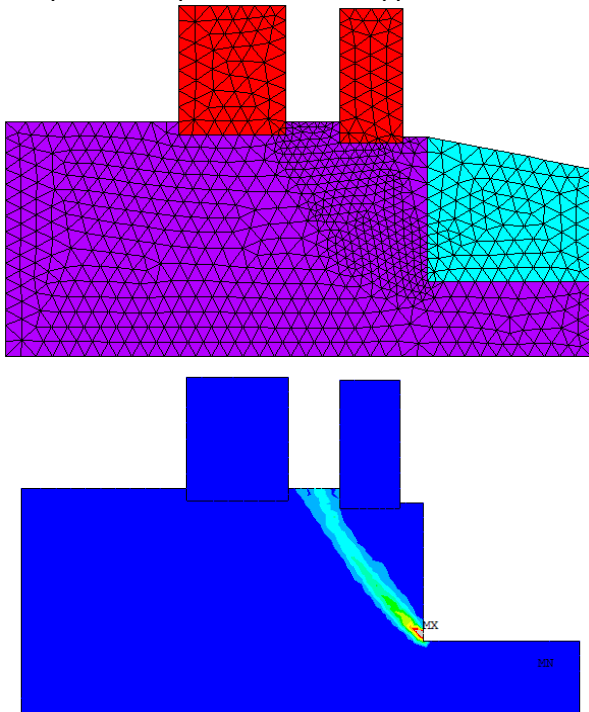


Fig. 7. Failure model without considering the structural plane

In addition, numerical analysis has shown that there was about 9 mm displacement without reinforcement after slope excavation as shown in Figure 8. It may cause crack in the existing old building.

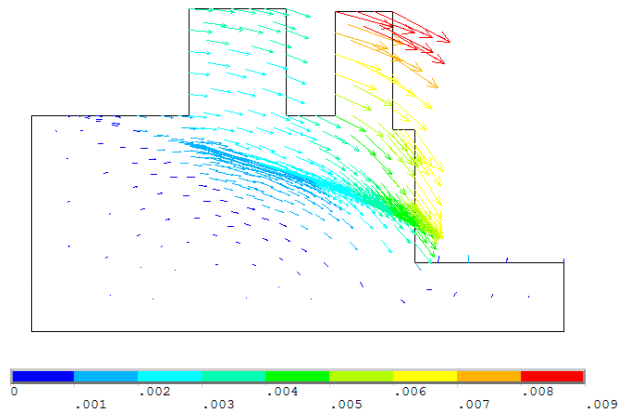


Fig. 8. The displacement vector of element after excavation

### C. The Lateral Loads Calculation

The cross-section area of anchor cable was determined by the corresponding lateral loads. The support structure was designed based on maximum lateral loads during the most unfavourable situation. Adjacent building load was considered as the overload of 15kPa each floor. The calculated results are shown as follows taking an example of 1-1 cross section.

(1) According to the failure model of sliding along sandstone and mudstone contact surface, the calculated result of lateral loads was  $Ea1=1268\text{kN/m}$  using the limit equilibrium method. The Chinese technical code for building slope engineering suggest that the lateral loads should be multiplied by a load factor of 1.3 when there are outward dipping structural plane and adjacent building. So, the modified lateral loads  $Ea1m$  was  $1648\text{ kN/m}$ .

(2) According to the Coulomb failure model without considering the structural plane and using the equivalent internal friction angle  $=55^\circ$ , the calculated result of lateral loads  $Ea2$  was  $669\text{kN/m}$ .

(3) According to the lateral at-rest pressure theory, the lateral loads was calculated by lateral at-rest pressure coefficient using Poisson's ratio.

$$E_0 = \frac{1}{2} r H^2 K_0 = 2928\text{kN/m} \quad (3)$$

$$K_0 = \frac{\mu}{1-\mu} \quad (4)$$

Where  $K_0$  is the lateral at-rest pressure coefficient.  $\mu$  is the Poisson's ratio.

Obviously,  $E_0$  is the maximum value among the three calculation results. So, the piles and anchor cable were designed base on the maximum lateral loads  $2928\text{kN/m}$ .

### D. The design scheme of support structure

According to the failure mode, if there is no strong support timely, the excavation will cause deformation and affect the safety of existing old building. Deformation control is often as critical as assurance against collapse. The challenges to limit the displacements or strains become the key factors of support structure selection. Therefore, the stabilizing piles strengthened by a series of tie-back anchor cable were designed to protect the cut slope as shown in Figure 9.

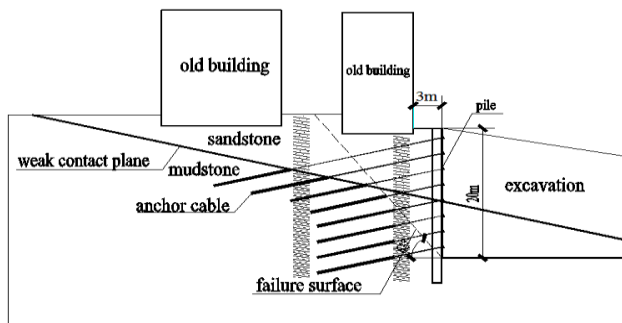


Fig. 9. The Scheme of supporting structure

The design scheme were required to construct the pile at first, and then construct the pre-stressed anchor cable on the piles step by step according to the top down construction sequence. The rectangular pile with the size of  $1.0 \times 1.2\text{m}$  was designed by artificial construction method. Anchor cable should be constructed as soon as possible immediately after excavation. The next stage slope can't be excavated until the former stage anchor cable begin to work. The anchor cable can't be pulled and locked until the strength of the pile concrete and anchorage segment mortar reach 90% of design strength.

#### E. The Considered Intelligent Monitoring System Model

The integrated control device is the core of the monitoring system and has the function of communication, which can realize the power supply protection of the equipment and the monitor various states of the equipment.

The device uses modular components for standardized production. The system composition of the monitoring system is the basic skeleton of the entire monitoring system. Select the corresponding organizational structure according to the actual needs of the system, make full use of the current Internet platform resources, and reduce software development costs. The building electrical equipment monitoring system uses home broadband, which breaks through the actual functions of traditional buildings in the current society, and can also make people more and more closely connected, realize real-time monitoring, and facilitate the dissemination of data. Because the B/S mode data monitoring system is developed externally, when designing the system, first of all, it must be clear that the external network of the system is safe and reliable, and secondly, the data transmission efficiency of the system must be high, and the real-time performance must be accurate. Finally, the design of the monitoring system should follow the requirements of international standards, so that the system is open to the outside world, and the design of the monitoring system should be operational and practical.

#### F. The Effects of Construction Sequence

According the construction plans, it need to take long time to construct the pile and anchor cable. But the investment units wanted to speed up the construction. They hoped to start the excavation early so that they could start the building foundation construction. So, they start the excavation of foundation pit at a horizontal distance of 15 meters from the slope as shown in Figure 10. The pile and anchor cable was

under construction at that time and not working. They thought that the rock slope was stable by their personal experience. However, it caused the slope deformation and cracks in a existing kindergarten building wall as shown in Figure 11. It threatened the safety of the residents and kids in the kindergarten seriously. The kindergarten was forced to relocated, and got compensation.



Fig. 10. The construction site photos



Fig. 11. The crack in old building wall



Fig. 12. The slope collapse site

Surface displacement of the slope was monitored by Chongqing rock and soil engineering test center. Twelve



monitoring points were set and has monitored for two years. The monitoring results shown the displacement was very small while the top down construction sequence was followed strictly. The horizontal displacement of total value was less than 5 mm. On the other hand, the maximum displacement was up to 33mm while the top down construction sequence wasn't followed. Figure 13 is the site photo during construction.



Fig. 13. The site photo during construction

#### IV. CONCLUSIONS

Case study of the vertical slope excavation near existing buildings based on visual monitoring of intelligent robots is conducted in the paper. For the slope excavation and supports adjacent to existing buildings, the bracing system must meet both ultimate and serviceability limit state requirements. Stability safety factor can be calculated using traditional limit equivalent method. It is difficult to accurately predict the deformations caused by the excavation using numerical analysis. The constitutive model used to simulate rock and soil behavior is a key problem. The commonly used elastic-perfectly plastic constitutive models are not adequate for estimating deformations. This paper introduced an empirical method for the high cut slope in China through a case study.

Engineering practice has shown that piles combined with pre-stressed cable anchor is a safe and reliable supporting structure. It is especially suitable for the soil cut slope or III, IV class rock cut slope which is close to the existing building. The lateral loads acting the anchor cable and piles are determined by maximal value of the at-rest pressure and modified active pressure.

It is difficult to predict the accurate time of slope collapse after excavation. For some hard rock slope, it can stand for a long time on their own without support. Some cut slope collapsed after several days or half a month and even half a year. The top-down construction sequence is an important construction method. The Chinese technical code for building slope engineering require that class III & IV rock slope construction should follow the top-down construction sequence strictly. For class II rock slope, it needs to consider the horizontal distance between the slope cutting line to the top of building foundation edge, height of slope, engineering level of risk etc.

#### V. ACKNOWLEDGEMENT

The authors acknowledge the financial support of Chongqing Basic Research and Frontier Exploration Project(CSTC2018JCYJAX0373) .

#### REFERENCES

- [1] Ou, C. Y., Liao, J. T. and Cheng, W. L. 2000. Building response and ground movements induced by a deep excavation. *Geotechnique*, 50(3): 209-220.
- [2] Long, M. 2001. Database for retaining wall and ground movements due to deep excavations. *Journal of Geotechnical and Geo-environmental Engineering*, 127,(3):203-224.
- [3] Finno, R. J. and Bryson, L. S. 2002. Response of building adjacent to stiff excavation support system in soft clay. *Journal of Performance of Constructed Facilities*, 16(1): 10-20
- [4] Liu, G. B., Ng, C. W. W. and Wang, Z. W. 2005. Observed performance of a deep multistrutted excavation in Shanghai soft clays. *Journal of Geotechnical and Geoenvironmental Engineering*, 131(8): 1004-1013.
- [5] Liu, G. B., Jiang, R. J., Ng, C. W. W. and Hong, Y. 2011. Deformation characteristics of a 38 M deep excavation in soft clay. *Canadian Geotechnical Journal*, 48(12): 1817-1828.
- [6] Ng, C. W. W., Hong, Y., Liu, G. B. and Liu, T. 2012. Ground deformations and soil-structure interaction of a multi-propped excavation in Shanghai soft clays. *Geotechnique*, 62(10): 907-921.
- [7] Simpson, B. N. D., Banfi, M., Grose, B., Davies, R. 2008. Collapse of the Nicoll Highway Excavation, Singapore. 4th International Conference on Forensic Engineering, London, UK, ICE.
- [8] Korff, M. 2009. Deformations and damage to buildings adjacent to deep excavation in soft soils. Literature survey - 1001307-004-GEO-0002.
- [9] Lo, K. Y. 2011. The effects of deep excavations in soils and rock on adjacent structures. The 14th Pan-American Conference on Soil Mechanics and Geotechnical Engineering (PCSMGE), the 64th Canadian Geotechnical Conference (CGC). Toronto, Ontario, Canada.
- [10] Finno, R., Voss, F., Rossow, E. and Blackburn, J. 2005. Evaluating Damage Potential in Buildings Affected by Excavations. *Journal of Geotechnical and Geo-environmental Engineering*, 131(10): 1199-1210.
- [11] Dinakar K. N., Prasad S. K. 2014. Effect of deep excavation on adjacent buildings by diaphragm wall technique using PLAXIS. *OSR Journal of Mechanical and Civil Engineering*, 26-32.
- [12] Miedzialowski C., Siwik D. 2014. The Impact of Deep Foundations of Building Structures on the Neighbouring Buildings – a Static Analysis. *American Journal of Civil Engineering and Architecture*, 2(4):136-142.
- [13] Dong, Y. 2014. Advanced Finite Element Analysis of Deep Excavation Case Histories. PhD Thesis. University of Oxford.
- [14] Dawson, E. M. Roth, W. H., Drescher, A. 1999. Slope stability analysis by strength reduction. *Geotechnique*, 49(6): 835-40.
- [15] Griffiths, D. V., and Lane, P. A. 1999. Slope stability analysis by finite elements. *Geotechnique*, 49(3):387-403.
- [16] Khan, Ameer Tamoor, Shuai Li, and Xinwei Cao. "Control framework for cooperative robots in smart home using bio-inspired neural network." *Measurement* 167 (2021): 108253.
- [17] Arents, Janis, and Modris Greitans. "Smart Industrial Robot Control Trends, Challenges and Opportunities within Manufacturing." *Applied Sciences* 12, no. 2 (2022): 937.
- [18] Abate, Andrea F., Paola Barra, Carmen Bisogni, Lucia Cascone, and Ignazio Passero. "Contextual trust model with a humanoid robot defense for attacks to smart eco-systems." *IEEE Access* 8 (2020): 207404-207414.
- [19] Qu, Ying, Petar Durdevic, and Zhenyu Yang. "Smart-spider: Autonomous self-driven in-line robot for versatile pipeline inspection." *Ifac-papersonline* 51, no. 8 (2018): 251-256.
- [20] Pane, Yudha P., Subramanya P. Nagesh Rao, Jens Kober, and Robert Babuška. "Reinforcement learning based compensation methods for robot manipulators." *Engineering Applications of Artificial Intelligence* 78 (2019): 236-247.

- [21] Chen, Yulin, Hailing Sun, Guofu Zhou, and Bao Peng. "Fruit Classification Model Based on Residual Filtering Network for Smart Community Robot." *Wireless Communications and Mobile Computing* 2021 (2021).
- [22] Lu, Yuqian, Chao Liu, I. Kevin, Kai Wang, Huiyue Huang, and Xun Xu. "Digital Twin-driven smart manufacturing: Connotation, reference model, applications and research issues." *Robotics and Computer-Integrated Manufacturing* 61 (2020): 101837.
- [23] Sim, H. S., M. S. Kim, M. H. Choi, H. Y. Bae, H. J. Kim, D. B. Kim, and S. H. Han. "A Study On Intelligent Robot Control Based On Voice Recognition For Smart FA." *Journal of the Korean Society of Industry Convergence* 21, no. 2 (2018): 87-93.
- [24] Fan, Fei, Gongping Wu, Man Wang, Qi Cao, and Song Yang. "Robot delay-tolerant sensor network for overhead transmission line monitoring." *Applied Sciences* 8, no. 6 (2018): 847.
- [25] Mahieu, Christof, Femke Ongenaes, Femke De Backere, Pieter Bonte, Filip De Turck, and Pieter Simoens. "Semantics-based platform for context-aware and personalized robot interaction in the internet of robotic things." *Journal of Systems and Software* 149 (2019): 138-157.
- [26] Rodić, Aleksandar, Ilija Stevanović, and Miloš Jovanović. "Smart cyber-physical system to enhance flexibility of production and improve collaborative robot capabilities-mechanical design and control concept." In *International Conference on Robotics in Alpe-Adria Danube Region*, pp. 627-639. Springer, Cham, 2018.
- [27] Wan, Jiafu, Jun Yang, Zhongren Wang, and Qingsong Hua. "Artificial intelligence for cloud-assisted smart factory." *IEEE Access* 6 (2018): 55419-55430.
- [28] Chen, Zhenyi, Kwang-Cheng Chen, Chen Dong, and Zixiang Nie. "6G Mobile Communications for Multi-Robot Smart Factory." *Journal of ICT Standardization* (2021): 371-404.
- [29] Mizumaru, Kazuki, Satoru Satake, Takayuki Kanda, and Tetsuo Ono. "Stop doing it! Approaching strategy for a robot to admonish pedestrians." In *2019 14th ACM/IEEE International Conference on Human-Robot Interaction (HRI)*, pp. 449-457. IEEE, 2019.
- [30] Wang, Le, Shengquan Xie, Wenjun Xu, Bitao Yao, Jia Cui, Quan Liu, and Zude Zhou. "Human Point Cloud Inpainting for Industrial Human-Robot Collaboration Using Deep Generative Model." In *International Manufacturing Science and Engineering Conference*, vol. 84263, p. V002T07A023. American Society of Mechanical Engineers, 2020.